NOTES AND CORRESPONDENCE

On Recirculation Forced by an Unstable Jet*

STEVEN R. JAYNE AND NELSON G. HOGG

Woods Hole Oceanographic Institution, Woods Hole, Massachusetts

10 September 1998 and 9 February 1999

ABSTRACT

Previous numerical experiments with an unstable zonal jet on a β plane are extended to the reduced-gravity case. The strength of the resulting recirculation varies inversely with the combination $\beta + 1/S$ where S is the Burger number and β the latitudinal variation of the Coriolis parameter. In addition, the centers of the antisymmetrically located gyres are located a distance from the jet inlet that varies inversely with the linear growth rate of small perturbations. An improved analytic model has also been constructed that predicts the recirculation strength and has the single unsupported assumption that the meridionally integrated potential vorticity anomaly be independent of zonal position.

1. Introduction

Western boundary currents exhibit the phenomenon of recirculation through which the downstream transport of water is increased manyfold by flanking, weakly depth-dependent gyres (e.g., Richardson 1985; Hogg et al. 1986; Schmitz and McCartney 1993). The essential physics of these gyres has been the subject of much speculation with possibilities ranging from purely inertial flow following closed contours of potential vorticity (Hogg and Stommel 1985), to forcing by eddy form drag resulting from baroclinic instability in the westward moving Sverdrup flow (Rhines and Holland 1979), to more direct driving by eddies in the jet, itself (e.g., Haidvogel and Rhines 1983; Cessi et al. 1987; Spall 1994; Jayne et al. 1996).

In a recent paper (Jayne et al. 1996) we reported on a series of numerical experiments with a barotropic, quasigeostrophic, β-plane model that combines features of both the inertial and direct eddy forcing schools of thought. Entering from the western boundary of the rectangular domain, a zonal jet becomes unstable if it is sufficiently narrow. As the instabilities grow they smooth out the potential vorticity (pv) anomaly of the incoming flow both by transferring pv across the jet axis and by building plateaus of more or less uniform pv to the north and south of the jet. Once these terraces are established, recirculating gyres with closely inertial dynamics result. Under certain assumptions, some well based in theory, some ad hoc, we were able to develop an analytic model that predicted, reasonably well, the dependence of recirculation transport on the single environmental parameter, β, the nondimensional variation of Coriolis parameter with latitude.

After briefly describing the numerical model (section 2) we will present extensions to the barotropic case that put the analytic model on a somewhat better footing (section 3), although there remains one assumption that is based on empirical results alone with no theoretical basis of which we are aware. We will also show how these arguments work when extended to the simplest baroclinic situation: the reduced gravity case (section 4). Conclusions are given in section 5.

2. The numerical model

The model is essentially the quasigeostrophic one described in Jayne et al. (1996) with the principal changes being to make it nondimensional and to add the facility to deal with the reduced gravity case. We solve the potential vorticity equation:

$$\frac{\partial q}{\partial t} + J(\psi, q) = -R\nabla^2\psi \tag{1}$$

with

$$q = \nabla^2\psi - \frac{\psi}{S} + \beta y,$$

ψ being the streamfunction, S the square of the ratio of

* Woods Hole Oceanographic Institution Contribution Number 9803.

Corresponding author address: Dr. Nelson G. Hogg, Woods Hole Oceanographic Institution, Woods Hole, MA 02543.
E-mail: nhogg@whoi.edu

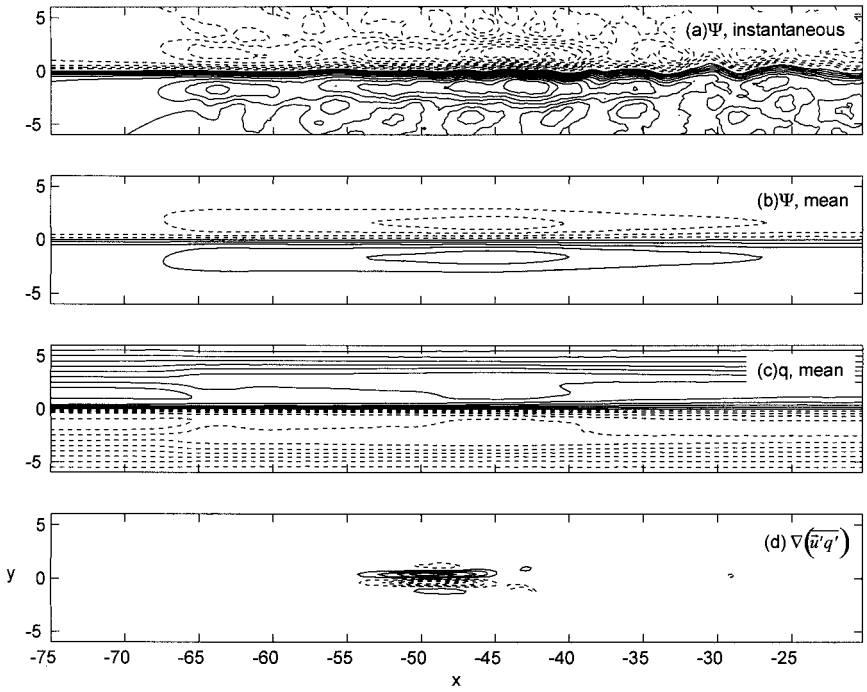

FIG. 1. The barotropic case with $\beta = 0.5$. (a) Instantaneous (contour interval 0.1) and (b) time averaged streamfunction (0.2) as well as the time-averaged (c) potential vorticity (0.25) and (d) the divergence of its flux by eddies (0.005) are shown in a strip that contains only a portion of the full domain ($-75 < x < 75$, $-40 < y < 40$). Negative values of the quantities are dashed.

the Rossby radius of deformation to the jet width (the Burger number), and R a nondimensional bottom friction coefficient. The inflow is specified at the western boundary, $x = x_W$, by

$$\psi(x_W, y) = \begin{Bmatrix} +\frac{1}{2}, & y < -1 \\ -\frac{1}{2}\left(y + \frac{\sin(\pi y)}{\pi}\right), & |y| < 1 \\ -\frac{1}{2}, & y > 1 \end{Bmatrix}, \quad (2)$$

with a similar condition on the outflowing, eastern boundary but with the width of the outflowing jet adjusted to give marginal stability there, as described below. The initial condition is essentially (2) extended to all x. Equation (1) is then integrated in time and space using a scheme that is center differenced in the two space dimensions and forward stepped in time using a third-order Adams–Bashforth scheme (Durran 1991). Advective terms are handled using the vorticity conserving scheme of Arakawa (1966). Dissipative sponge layers, 50 grid points wide, are placed next to all the boundaries to absorb waves and other time-dependent motions radiated by the meandering, unstable jet. Away from the sponge layers the explicit friction, $R = 10^{-4}$, is chosen to be as low as possible, consistent with numerical stability (dimensional values for the dissipation time scale range from 16 years at $\beta = 0.05$ to 600 years at $\beta = 2$). The nondimensional grid spacing is 0.2 (i.e., there are 10 grid points in the inflowing jet) and the number of grid points is 751 (E–W) by 401 (N–S) including the buffer zones. With the origin at the center of the domain this gives $x_W = -75$ and the northern boundary at $y = 40$ nondimensional units.

3. The barotropic case ($S = \infty$)

a. Numerical model results

We have made a number of model runs to determine the dependence of the recirculating transport on β and the sensitivity of the results to other subjective choices such as the shape of the inflowing jet. As will be seen in section 3b, the jet described by (2) satisfies the necessary condition for instability when $\beta < \pi^2/2$. In this unstable regime the model is run until it has come into equilibrium and then for a further period over which time-averaged statistics are computed. A typical case is shown in Fig. 1. Here $\beta = 0.5$ and the jet enters through the western wall and, because of the two extrema in the pv distribution (Fig. 1c), becomes unstable. The instabilities smooth out these extrema, erode terraces into the pv field away from the jet (Fig. 1c), and smooth out the jet itself. Within the terraces nearly inertial, counterrotating gyres are set up (Fig. 1b) in which weak eddy forcing is balanced by weak dissipation. For this example the strength of these gyres is about 0.4, as

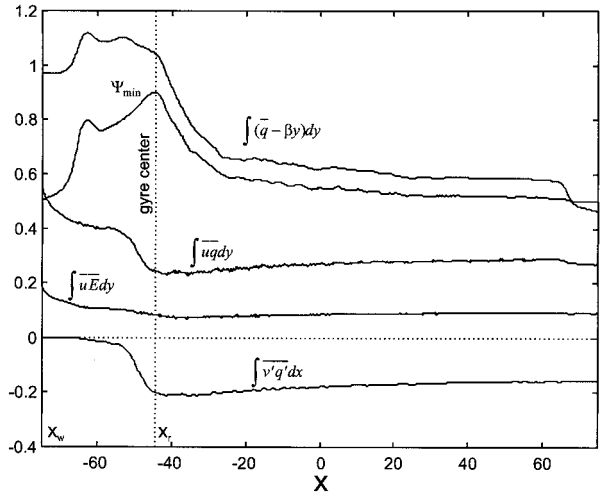

FIG. 2. Zonal distributions of various quantities, as indicated, for the barotropic case with $\beta = 0.5$.

determined by subtracting the value of the streamfunction at the jet edge (0.5) from its extremum (0.9). In other words, each recirculation gyre carries about 40% of the transport of the jet itself.

The divergence of the eddy pv flux is most prominent just upstream of the gyre centers at the end of the region where the jet is most unstable and then dies quickly (Fig. 1d). This suggests that the region from this point on is only weakly affected by eddy fluxes, an idea that is confirmed by computation of the along current variation of the meridional integrals of the zonal fluxes of pv and energy by the mean flow (Fig. 2). Both diminish upstream of the gyre center and then change little through the remainder of the domain. Along the jet axis the cumulative southward flux of pv by the eddies has a similar behavior.

Eddy fluxes have a profound affect on the relationship of q and ψ (Figs. 3a,c). At the inflow ($x = x_w$) this dependence is specified by (2) and is very nonlinear but by the point of maximum recirculation ($x = x_r$) it has

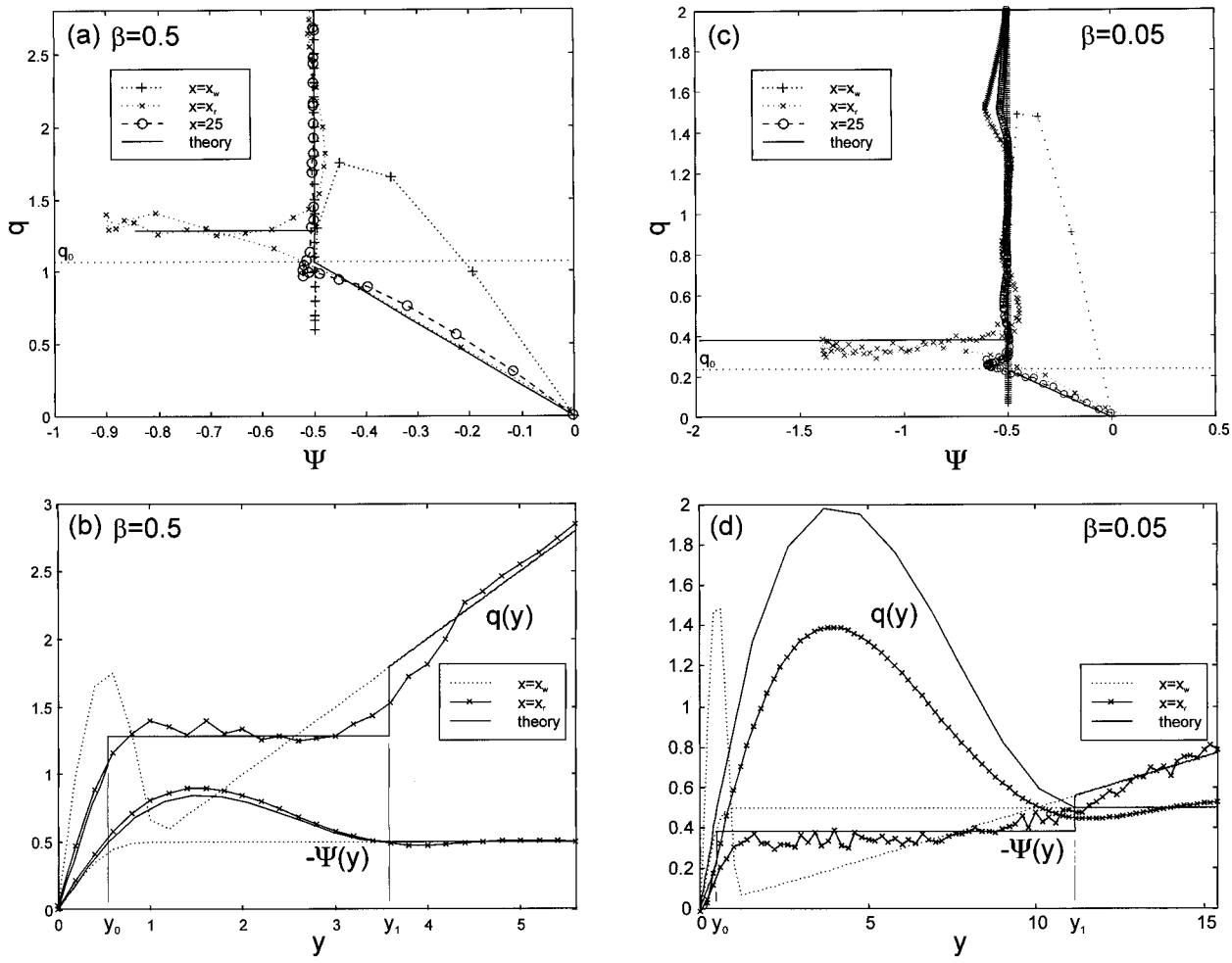

FIG. 3. Potential vorticity vs (a) and (c) streamfunction and (b) and (d) meridional distance for the barotropic case with $\beta = 0.5$ (a) and (b) and $\beta = 0.05$ (c) and (d) at four locations along the channel. Only the northern half of the domain is plotted. The longitude of the inlet is x_w and the point of maximum recirculation is x_r.

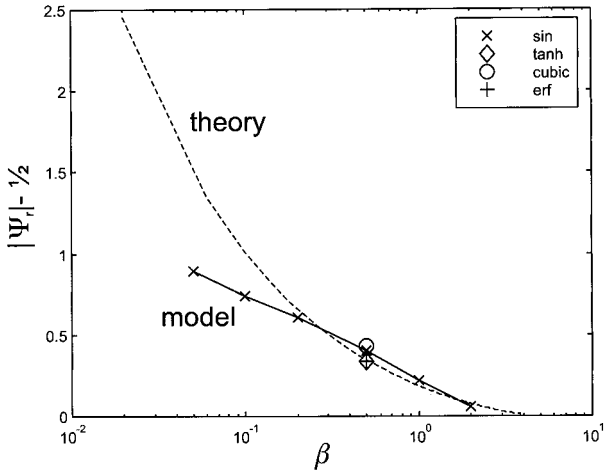

FIG. 4. Recirculation strength as a function of β for the barotropic case. Points give experimental values while the solid curve shows the theoretical prediction. In addition to the standard sine function jet several other analytic shapes, as indicated, were run with $\beta = 0.5$. All were chosen to have the same transport and maximum speed.

become approximately piecewise linear: linear in the region of the jet, constant pv through the recirculation, and constant ψ beyond. The smoothing tendency of the eddies is apparent in the meridional distribution of q (Figs. 3b,d): the large positive anomaly advected in through the western boundary north of the jet axis is redistributed to make a more monotonic distribution with a level plateau within the gyre. The plateau shrinks to the east and finally vanishes to leave a jet of marginal stability (i.e., q_y vanishes at the jet's edge but does not change sign).

The recirculating transport is a strongly decreasing function of β (Fig. 4). Most of our experimentation has been done using the ''sine'' jet but we also ran the $\beta = 0.5$ case using three other analytic forms for the streamfunction at the inflow: a hyperbolic tangent (the ''Bickley'' jet), an error function, and a cubic polynomial of odd powers only. Each of these had unit amplitude for the nondimensional velocity at the jet axis and the same total transport. Their resulting recirculations are almost identical to that for the sine jet (Fig. 4).

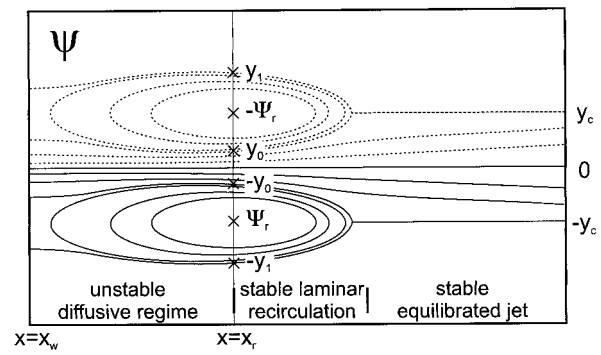

FIG. 5. Schematic showing an idealization of the different physical regimes existing along the channel.

b. Quasi-analytic model

The results of the numerical experiments have inspired us to consider an idealized representation of the physics in which the domain is broken into three distinctly different regimes (Fig. 5). Between the western boundary and the center of the recirculation gyres is the unstable portion of the jet in which eddy flux divergences rearrange the pv to develop the homogenized terraces around which the recirculating gyres set up. Beyond this point the eddies subside and the flow becomes more closely laminar with energy and pv conserved (e.g., Fig. 2). Weak meridional flow feeds the eastern limbs of the recirculations until continuity is satisfied and then the jet continues to the outflow in a marginally stable configuration. We will deal with each of these regimes in reverse order.

A striking feature of the numerical results is the linearization of the relationship between q and ψ (e.g., Fig. 3), a seemingly common feature of experiments with quasigeostrophic eddy-resolving physics (e.g., Marshall 1984; Griffa and Salmon 1989). Turbulent flow coming to equilibrium over random topography tends to conserve its energy but dissipates enstrophy because its spectrum is much ''bluer'' than that of energy. Statistical methods (Salmon et al. 1976) and variational calculus (Bretherton and Haidvogel 1976) both conclude that a linear relationship between pv and streamfunction should result. Griffa and Salmon (1989) have extended this result, numerically, to situations without topography but with forcing and dissipation. Similar physics appear to be at work in our experiments, at least within the unstable jet. Although the flow field is far from homogeneous, the eddy processes working in the unstable region of the jet act to dissipate enstrophy more rapidly than energy, and the jet then evolves in space and time into one with the linear q–ψ functional form.

Within the jet, downstream of the recirculations, x derivatives can be neglected in favor of those in the y direction and the assumed linear q–ψ relationship can then be written

$$\psi_{yy} + \beta y = q = -2q_0\psi, \tag{3}$$

where $q = \pm q_0$ is the value of q at the edge of the jet, $y = \pm y_c$ say, where $\psi(x, \pm y_c) = \mp\frac{1}{2}$. Equation (3) is a linear ODE and, if we assume that ψ antisymmetric, there are three unknowns, $q_0 y_c$ and an integration constant. One condition is obtained from $\psi(x, y_c) = -\frac{1}{2}$ and another from the vanishing of u at the edge of the jet [$u(x, y_c) = -\psi_y(x, y_c) = 0$]. For the third we assert that the jet is marginally stable implying that $q_y = q_{yy} = 0$ at some point within the jet. These conditions give

$$q_0 = \frac{(2\beta\pi)^{2/3}}{2},$$

$$\psi(x, y) = -\frac{1}{2}\left(\frac{y}{y_c} + \frac{\sin(\pi y/y_c)}{\pi}\right), \qquad |y| < y_c, \quad (4)$$

$$y_c = \left(\frac{\pi^2}{2\beta}\right)^{1/3},$$

and the point where q_y and q_{yy} vanish is at $y = \pm y_c$. With (4), and the conditions $q = \beta y$, $\psi = \pm$½ exterior to the jet $q(\psi)$ is a piecewise linear function which the model jet closely follows (see curves for $x = 25$ in Figs. 3a,c).

Equation (4) has a similar form to that for the incoming jet [see Eq. (2)]. If we set $y_c = 1$ to make them identical, we deduce that

$$\beta < \beta_c \equiv \frac{\pi^2}{2}$$

is the necessary condition that must be satisfied for the incoming flow to be barotropically unstable.

We expect (3) and the same linear q–ψ relationship to hold within the jet in the laminar recirculation region (Fig. 5), that is, everywhere downstream of the maximum recirculation point. However, in this region the jet is flanked by the gyres rather than quiescent fluid and the boundary conditions will change, although the constant of proportionality in the q–ψ relationship, q_0, will not. The solution to (3) is now

$$\psi(x_r, y) = -\frac{y}{2y_c} + A \sin\left(\frac{\pi y}{y_c}\right), \qquad |y| < y_0, \quad (5)$$

where $x = x_r$ is the abscissa of the gyre center and A and y_0 are unknown constants with the latter representing the outer limit of the part of the eastward flow that is continuous with the equilibrated jet farther downstream (Fig. 5).

Within the recirculation we assume that pv is homogenized, an assumption that is well supported by the numerical work (Fig. 3) and has a solid theoretical basis (Rhines and Young 1982). The level at which pv homogenizes, however, is unknown and for now we will treat it as a constant $\overline{q}$, yet to be determined. One might presume that the pv distribution would be continuous at the boundaries between the jet and the recirculation gyres so that $\overline{q} = q_0$. However, within the context of this laminar model we can think of no a priori justification for this assumption and our experiments (e.g., Fig. 3a) suggest that the homogenized level, $\overline{q}$, is different from q_0. In addition, if we were to assume continuity of q, it can be shown that the recirculation strength becomes independent of β, in disagreement with the numerical experiments (Fig. 4). Therefore, within the gyres

$$\psi_{yy} + \beta y = \overline{q}, \qquad y_0 < y < y_1, \quad (6)$$

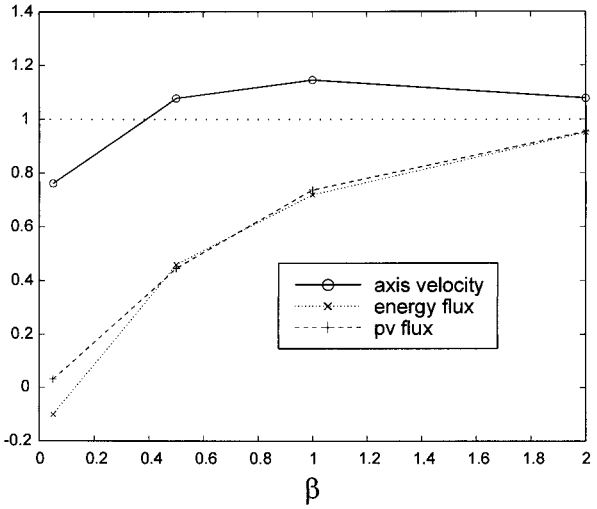

FIG. 6. Ratio of axis velocity, energy flux, and pv flux at the point of maximum recirculation to their values at the inlet as a function of β.

where $y = y_1$ is the northern extremity of the gyre and we again favor y derivatives at the expense of those in the x direction. With further stipulations that $\psi(x_r, y_0) = \psi(x_r, y_1) = -$½, and $u(y_1) \equiv -\psi_y(y_1) = 0$, and some algebra it can be shown that

$$\psi(x_r, y) = -\frac{1}{2} - \frac{\pi^2}{12y_c^3}(y - y_0)(y_1 - y)^2, \quad y_0 < y < y_1, \quad (7)$$

and

$$\overline{q} = \beta\frac{y_0 + 2y_1}{3}.$$

Two additional conditions can be obtained for the remaining three unknowns (A, y_0, and y_1) by matching velocity and streamfunction at $y = y_0$:

$$A \sin\left(\frac{\pi y_0}{y_c}\right) = \frac{(y_0 - y_c)}{2y_c},$$

$$A \cos\left(\frac{\pi y_0}{y_c}\right) = \frac{6y_c^2 - \pi^2(y_1 - y_0)^2}{12\pi y_c^2}. \quad (8)$$

These equations are further reducible to a single transcendental equation relating y_1 and y_0:

$$y_1 = y_0 + \sqrt{6}\frac{y_c}{\pi}\left(1 + \frac{\pi(y_c - y_0)}{y_c \tan(\pi y_0/y_c)}\right)^{1/2}. \quad (9)$$

We need one remaining condition to close the problem, and this one will have to link the laminar regime with the inflow. Failing to deduce any invariant of the flow that might be invoked to make this connection we have resorted to empirical evidence. In Fig. 2 we show, for $\beta = 0.05$, the longitudinal distributions of several quantities that one might expect to be conserved: energy flux, vorticity flux, and, based on our previous work

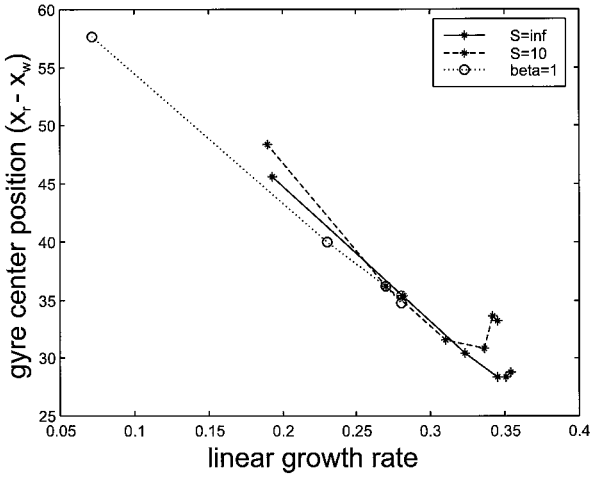

FIG. 7. Zonal position, $x_r - x_W$ of the center of the recirculation gyres, defined as the position of the extremum in streamfunction, as a function of linear growth rate of small sinuous perturbations to the inflowing jet. Two values of Burger number (with β varied) and one of β (with S varied) are shown.

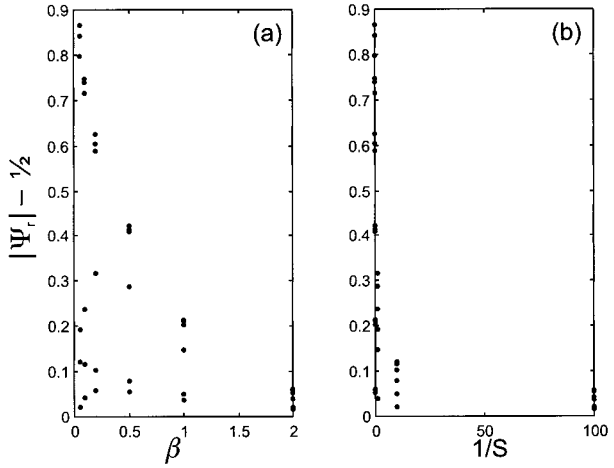

FIG. 8. Recirculation strength plotted vs (a) β and (b) $1/S$ for all of our experiments with the reduced-gravity case.

(Jayne et al. 1996), the jet axis velocity. The last of these is most nearly constant between the jet entrance and the gyre center, especially for β not too far from β_c (Fig. 6). An alternate way of expressing this condition, which we will find more appropriate in the reduced gravity case to follow, is that the integrated pv anomaly, defined as $\int_0^\infty (q - \beta y)\, dy \approx \int_0^\infty \psi_{yy}\, dy = u(x, 0)$, is independent of longitude. This yields

$$A = \frac{1 - 2y_c}{2\pi} \tag{10}$$

from (5) and the problem is now closed. The resulting solutions for $q(\psi)$, $q(y)$ and $\psi(y)$ are superimposed on the numerical results in Fig. 3 and are satisfyingly close to the mark.

Our primary interest is in being able to predict the strength of the recirculation or equivalently the extreme value of $\psi(x, y)$, ψ_r say, given β. Differentiation of (7) to find the position of the extremum and then substitution back into (7) gives

$$\psi_r = -\frac{1}{2} - \frac{\pi^2}{81}\left(\frac{y_1 - y_0}{y_c}\right)^3$$

$$= -\frac{1}{2} - \frac{2}{81}\beta(y_1 - y_0). \tag{11}$$

The additional recirculating transport is equal to the absolute value of the second term on the right-hand side and is compared with the numerical results in Fig. 4. There is close agreement for $\beta > \sim 0.5$ but increasing disagreement for smaller values for which the jet becomes increasingly unstable.

The value of β determines the growth rate of the fastest growing small amplitude perturbations and it should come as no surprise that, in addition to the recirculation strength, the distance of the center of the recirculation gyre from the western boundary, $x_r - x_w$, is inversely dependent on this parameter (Fig. 7).

4. The reduced gravity case (finite S)

a. Preliminary considerations

Inspection of (1) will show that the extension to the reduced-gravity case involves the stretching contribution to the pv in the time-dependent term only, as it identically vanishes in the Jacobian. Therefore S does not appear explicitly in the time-averaged equations and the effects of stratification enter indirectly through its impact on the stability of the zonal jet and the dynamics of the resulting fluctuations. Taking the sine jet, once again, as the prescribed form of the inflow the condition for marginal stability remains $\beta = \pi^2/2$ and has no dependence on S. Nevertheless, it is clear that the time-dependent dynamics are sensitive to the stratification and, as we will show, so is their rectification into recirculation gyres.

b. Numerical model results

A large number of numerical runs have been made with different values of β and S and the results, in terms of the recirculation index, are shown in Fig. 8. As with the barotropic case, the strength of recirculation increases with decreasing β but now also with decreasing $1/S$. As both parameters are involved, we have attempted empirically to find a combined parameter that would collapse the results onto a single curve. Although not perfect the combination $\beta + 1/S$, based on the pv gradient at the axis of the inflowing jet $q_y(x_w,0) = \pi^2/2 + \beta + 1/S$, works quite well (Fig. 9).

c. Quasi-analytic model

Encouraged by our success with the barotropic case we have proceeded along the same path for this reduced-

gravity situation. With identical notation $\psi(x_w, y)$ takes the form of (5) in the region of the jet, $|y| < y_0$, although the constant of integration A will now be different. In the homogenized pv region,

$$\psi(x_r, y) = -\frac{1}{2} + \beta S(y - y_0) + B\left[\cosh\left(\frac{y - y_0}{\sqrt{S}}\right) - 1\right] + C \sinh\left(\frac{y - y_0}{\sqrt{S}}\right), \qquad y_0 < y < y_1. \quad (12)$$

As before, (5) and (12) describe the form of the streamfunction but now six constants need to be determined (y_0, y_1, $\overline{q}$, A, B, C). Five of these can be found from matching of ψ and ψ_y at y_0 (two conditions), setting $\psi = -\frac{1}{2}$ at y_0 and y_1 (two more) and making $\psi_y = 0$ at y_1, the outer edge of the recirculation. The resulting conditions can be combined and rearranged to give a solution sequence in terms of one unknown, y_0:

$$A = \frac{y_0 - y_2}{2y_c \sin\left(\frac{\pi y_0}{y_c}\right)},$$

$$C = -\frac{S^{1/2}}{2y_c}\left[1 + 2S\beta y_c - 2\pi A \cos\left(\frac{\pi y_0}{y_c}\right)\right],$$

$$B = \beta S^{3/2}\left(\frac{\sinh(\varsigma) - \varsigma\cosh(\varsigma)}{1 - \cosh(\varsigma)}\right),$$

$$\overline{q} = \beta y_0 + \frac{2B + 1}{2S}, \quad (13)$$

where $y_c = [\pi^2/(2\beta)]^{1/3}$ as before and $\varsigma = (y_1 - y_0)/\sqrt{S}$ is the solution of the hypergeometric equation:

$$1 - \frac{C}{\beta S^{3/2}} = \frac{\varsigma \sinh\varsigma}{\cosh\varsigma - 1}. \quad (14)$$

The remaining condition, once again, must be determined by connecting a property of the inflow with the recirculation.

For the barotropic case we used the condition that the axis velocity remains constant from the inflow to the point of fully developed recirculation. An alternative interpretation was that the meridionally integrated vorticity anomaly, $\int (q - \beta y,)\, dy$, was uniform. In the reduced-gravity situation these represent different conditions with the former giving (10), as before. For the latter the definition of the pv anomaly has to be extended to account for the effects of stratification. We choose to define it as

$$q_{\text{anomaly}} = q - \beta y - \frac{1}{2S}\,\text{sgn}(y)$$

so that the anomaly vanishes at large $|y|$. After considerable algebra the resulting condition is

$$y_c\left(2\beta y_c + \frac{1}{S}\right)\left\{\frac{y_0^2}{4y_c^2} + \frac{A}{\pi}\left[1 - \cos\left(\frac{\pi y_0}{y_c}\right)\right]\right\} + \overline{q}(y_1 - y_0) - \frac{\beta y_1^2}{2} - \frac{y_1}{2S} = 1 - \left(\frac{\pi^2 - 4}{4\pi^2 S}\right). \quad (15)$$

The constraint of Eq. (10) predicts a very weak dependence on β (not shown), whereas the integrated vorticity anomaly condition (15) gives surprisingly good agreement with the numerical experiments over a wide range of β and S (Fig. 9).

5. Discussion and conclusions

We have extended our earlier study of recirculation forced by an unstable jet on the β plane (Jayne et al. 1996) in several directions. First, we have performed experiments with a reduced-gravity model and studied the full two-dimensional parameter space provided by β and S, the Burger number. Although no new phenomena are found, the stability of the jet is sensitive to both parameters, but, rather surprisingly, we find that it depends principally on the combination $\beta + 1/S$, which is related to the pv gradient at the axis of the inflowing jet. By computing the growth rate of small amplitude perturbations we also find that the center of the recirculation gyre is located a distance from the western boundary that varies inversely with growth rate: the slower the growth rate the longer, in distance, it takes for the recirculation to develop (and the weaker it is).

We have also been able to put these results on a somewhat better theoretical footing. The potential vorticity homogenization theory of Rhines and Young (1982) supports the near constant values of pv found within the recirculation gyres. Statistical (Salmon et al. 1976; Griffa and Salmon 1989) and variational minimum enstrophy arguments (Bretherton and Haidvogel 1976) lend support to our empirically derived linear relationship between streamfunction and potential vorticity. With just one additional constraint we have been able to produce an analytic prediction for the gyre strength. One that works quite well is the constancy of the meridional integral of potential vorticity anomaly

$$q - \beta y - \frac{1}{2S}\,\text{sgn}(y),$$

but we have been unable to give a physical argument as to why this should be so.

Acknowledgments. Discussions with Paola Rizzoli have been helpful. We are grateful for the constructive remarks of the two anonymous reviewers. SRJ is supported by the Department of Defense under a National Defense Science and Engineering Fellowship and a Massachusetts Institute of Technology Climate Modeling Fellowship from the American Automobile Manu-

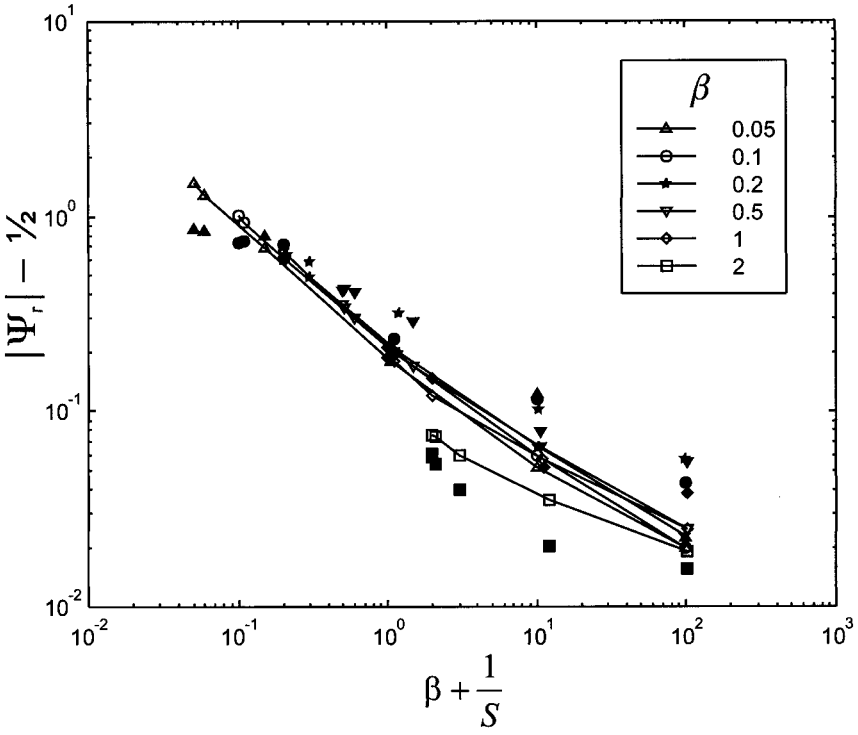

FIG. 9. Recirculation strength as a function of $\beta + 1/S$ for the reduced-gravity case, comparing the theoretical prediction (open symbols with solid line) with numerical results (solid symbols, no line).

facturers Association. NGH receives support through Grant N00014-96-1-0348 from the Office of Naval Research. Computational resources for the numerical simulations were provided by the National Center for Atmospheric Research, which is supported by the National Science Foundation.

REFERENCES

Arakawa, A., 1966: Computational design for long-term numerical integration of the equations of fluid motion: Part I: Two-dimensional incompressible flow. *J. Comput. Phys.*, **1,** 119–145.

Bretherton, F. P., and D. B. Haidvogel, 1976: Two-dimensional turbulence above topography. *J. Fluid Mech.*, **78,** 129–154.

Cessi, P., G. Ierley, and W. Young, 1987: A model of the inertial recirculation driven by potential vorticity anomalies. *J. Phys. Oceanogr.*, **17,** 1640–1652.

Durran, D. R., 1991: The third-order Adams–Bashforth method: An attractive alternative to leapfrog time differencing. *Mon. Wea. Rev.*, **119,** 702–720.

Griffa, A., and R. Salmon, 1989: Wind-driven ocean circulation and equilibrium statistical mechanics. *J. Mar. Res.*, **47,** 457–492.

Haidvogel, D. B., and P. B. Rhines, 1983: Waves and circulation driven by oscillatory winds in an idealized ocean basin. *Geophys. Astrophys. Fluid Dyn.*, **25,** 1–63.

Hogg, N. G., and H. Stommel, 1985: On the relation between the deep circulation and the Gulf Stream. *Deep-Sea Res.*, **32,** 1181–1193.

——, R. S. Pickart, R. M. Hendry, and W. J. Smethie Jr., 1986: The Northern Recirculation Gyre of the Gulf Stream. *Deep-Sea Res.*, **33,** 1139–1165.

Jayne, S. R., N. G. Hogg, and P. Malanotte-Rizzoli, 1996: Recirculation gyres forced by a beta-plane jet. *J. Phys. Oceanogr.*, **26,** 492–504.

Marshall, J. C., 1984: Eddy-mean-flow interaction in a barotropic model. *Quart. J. Roy. Meteor. Soc.*, **110,** 573–590.

Rhines, P. B., and W. R. Holland, 1979: A theoretical discussion of eddy-driven mean flows. *Dyn. Atmos. Ocean*, **3,** 289–325.

——, and W. R. Young, 1982: Homogenization of potential vorticity in planetary gyres. *J. Fluid Mech.*, **122,** 347–367.

Richardson, P. L., 1985: Average velocity and transport of the Gulf Stream near 55 W. *J. Mar. Res.*, **43,** 83–111.

Salmon, R., G. Holloway, and M. C. Hendershott, 1976: The equilibrium statistical mechanics of simple quasi-geostrophic models. *J. Fluid Mech.*, **75,** 691–703.

Schmitz, W. J., Jr., and M. S. McCartney, 1993: On the North Atlantic Circulation. *Rev. Geophys.*, **31,** 29–49.

Spall, M. A., 1994: Wave-induced abyssal recirculations. *J. Mar. Res.*, **52,** 1051–1080.